Trends in Applied Sciences Research

ISSN 1819-3579

Academic
Journals Inc.

www.academicjournals.com

Trends in Applied Sciences Research 2 (1): 1-14, 2007
ISSN 1819-3579

Construction of a Rational Delta Function Using the Reverse Cantor Set and its Application to Quantum Mechanics via Pseudo-spectral Methods

Aadel A. Chaudhuri
Department of Electrical Engineering and Computer Science,
Massachusetts Institute of Technology, Cambridge, MA 02139, USA

Abstract: A simple yet novel method for construction of rational delta function using the reverse Cantor set and its application to quantum mechanics is presented. This study is primarily concerned with introduction or derivation of some simple rational delta function that represents the orthonormality condition of the computed eigenfunctions — both in the physical space as well as the Fourier space — which will serve as the basis functions for the wave function, Ψ, the solution to the Shrödinger wave equation subjected to prescribed boundary conditions. The rational delta function, $\delta_n(x)$, based on a hitherto unavailable reverse Cantor set derived in this study, reduces to the Dirac δ-function and Kronecker δ-function in the limiting cases of $n \to \infty$ and $n \to 0$, respectively and thus bridges the gap between the two situations that arise in quantum mechanics, namely bound states with discrete eigenvalues and scattering case with continuous spectrum of eigenvalues. Most important, this novel rational delta function, $\delta_n(x)$, permits the resulting computed wave function to be expressed in the form of Discrete Fourier Transform (DFT) in the Fourier domain and recover the sampled wave function in the physical domain by employing the inverse discrete Fourier transform (IDFT). The example problem of a barrier inside a well studied here sheds new light on the nature of interaction of two or more potentials and will serve as a prelude to more complex many body interaction problems.

Key words: Shrödinger equation, Pseudo-spectral methods, Wave function, Reverse Cantor Set, Discrete Fourier Transform (DFT), Fast Fourier Transform (FFT), Discrete Wavelet Transform (DWT)

INTRODUCTION

Recent interests in nano-scale phenomena in diverse engineering fields, such as materials science, computer engineering, bioengineering, etc., have attracted increased attention to quantum mechanical studies by engineers. The modern quantum mechanics, first formulated simultaneously by Erwin Schrödinger and Werner Heisenberg around 1925, is a powerful theory that governs the propagation of electron waves (Schiff, 1968). Since both theories are analogous, only Schrödinger's theory will be considered in this study. Schrödinger's wave mechanics, which is based on linear operator theory and the corresponding eigenvalues and eigenfunctions, is quite general, governing the laws of wave motion which particles of any microscopic system must obey. Solution of the Schrödinger equation provides all the dynamical information on the physical system at the subatomic level. The basic postulates of quantum mechanics are reviewed in the Appendix in the interest of completeness of this investigation.

One basic idea pertaining to the wave function, ψ, which is a solution to the Schrödinger equation, is that unless ψ is normalized, computed values of important physical quantities, such as energy and momentum probability functions and expectation values would be meaningless. Furthermore, the wave function, ψ, can be expanded in terms of an orthonormal set of eigenfunctions,

which are orthonormalized with respect to one of the two forms of delta functions. If the wave function is localized as in the case of an infinite potential well, the computed eigenvalues are discrete and the eigenfunctions are orthonormalized with respect to Kronecker delta function. If, on the contrary, the wave function has a finite magnitude at great distances, such as those pertaining to the scattering case, the spectrum of eigenvalues is continuous and the corresponding eigenfunctions are orthonormalized with respect to Dirac delta function. The relevant mathematical details are reviewed in Section A.3, Appendix.

Although the wave motions of most systems involving microscopic particles, such as electrons, can be accurately modeled using the Schrödinger equation, the number of exact solutions are extremely limited. In problems pertaining to bound states, in which a particle is restrained by the external forces (potential energy) to a relatively localized region of space, giving rise to discrete eigenvalues, the exact or analytical solutions are limited by the relatively few potential energy functions and boundary conditions (i.e., the conditions that are a priori prescribed at the boundaries of the localized region) . Same is true for collision problems (i.e., collision of a particle with a force field), where the energy eigenvalues are continuously distributed. In this situation, the energy is specified in advance and the behavior of the wave function at great distances is found in terms of it. The asymptotic behavior of the solution is then related to the amount of scattering of the particle by the force field. These exact solutions are available in standard textbooks, such as Schiff (1968).

For most interesting practical problems, although the afore-mentioned exact solutions provide some clues to the approximate solutions, physicists and chemists must resort to some numerical methods, such as those based on the variational principle (Ritz method), stationary perturbation method, Feynman diagram method, WKB approximation, stationary collision theory, Born approximation, eikonal approximation, Hartree-Fock method, etc. (Schiff, 1968; Mattuck, 1992; Szabo and Ostlund, 1996). The most conventional approach has been based on obtaining stationary solutions subjected to prescribed boundary conditions (Asker, 1981). Time dependent solutions have been computed by expansion of the initial state in stationary solutions (Leasure *et al*., 1981). This stationary approach has produced efficient algorithms, that include the variational methods for bound states, close coupling methods (Wolken, 1973; Lill and Khouri, 1984) and R matrix methods for scattering states. In contrast, the direct time dependent approach such as the time dependent variational method due to Lee and Heller (1982) has the advantage of unifying the bound and scattering problems.

As has been discussed by Hoffman *et al*. (1998), for the Schrödinger equation with relatively simple boundary conditions, various spectral and pseudo-spectral methods (Feit and Fleck, 1983; Kosloff and Kosloff, 1983; Sharafeddin and Zhang, 1993; Wyatt, 1995) use standard basis functions, constructed from well-known polynomials such as Jacobi, Laguerre, Legendre, Hermite, Chebyshev and so on. These methods are highly accurate and can be implemented with a relatively small number of basis functions. The basic idea behind the method is to use the properties of the discrete Fourier transform to approximate spatial derivatives, while time derivatives have been approximated by differencing (Kosloff and Kosloff, 1983). The method maps the true Hilbert space of the problem to a discrete one. This mapping conserves the Hermitian quality and the commutation relations of the operators which are associated with actual observables (Kosloff and Kosloff, 1983).

With the advent of computers fast computational tools, such as the Fast Fourier Transform (FFT) method, the sinc method (Stenger, 1993) and the discrete wavelet transform method (Daubechies, 1992) have revolutionized fields of science and engineering in such diverse areas as radio astronomy, seismology, medical imaging, spectroscopy, compact disk technology, etc. All these fast computational methods are based on Discrete Fourier Transform (DFT) techniques. However, to the author's knowledge, the afore-mentioned quantum mechanics literature has not established a rigorous set theoretic basis for mathematical modeling via spectral and pseudo-spectral methods. The primary

objective of the present study is to bridge this long-standing gap. The fundamental step to solving this problem is concerned with (i) introduction or derivation of some simple rational delta sequences leading to corresponding delta functions in the limit and (ii) investigation of the fundamental set theoretic basis for formulation of these rational delta sequences. In what follows, formulation of a new type of rational delta function based representation theory for orthonormalization of the computed eigenfunctions both in the physical space as well as in the Fourier space, which will serve as the basis functions for the wave function, ψ, the solution to the Schrödinger wave equation subjected to prescribed boundary conditions, for particles in between bound states and scattering, will be presented. The specific goal of this investigation is to introduce a new rational delta function based on a hitherto unavailable reverse Cantor set derived in this study and to express the resulting computed wave function in the form of Discrete Fourier Transform (DFT) in the Fourier domain and recover the sampled wave function in the physical domain by employing the inverse Discrete Fourier Transform (IDFT). The transition to faster techniques, such as the Fast Fourier Transform (FFT) and Discrete Wavelet Transform (DWT), is relatively straightforward.

Reverse Cantor Set Based Delta Function

The Cantor Set, first formulated by George Cantor in 1883, is an important concept in the field of fractals. The Cantor set can be physically visualized as the removal of smaller and smaller segments from a line of some prescribed length (say unit length). The construction of the Cantor middle-thirds set proceeds by first taking a line segment of length 1, subdividing it into three segments and discarding the middle segment (middle third). This results in increasing the total number of line segments to two and decreasing the total length by 1/3 (to 2/3) at the end of each iteration. This process is continued recursively for the remaining line segments during second, third and subsequent iterations. In each subsequent step, the middle third of each segment is disposed of, thus creating twice as many segments as were previously present. In this operation, when carried to a limit of the number of iterations approaching infinity, the total length of the line segments clearly approach zero (a set of measure zero). In the mathematical language, these line segments then reduce to a fractal set of points on the line with a fractal dimension (a noninteger dimension) of ln 2/ln 3, which is between 0 and 1 (Moon, 1992; Devany, 1989). A fractal is a set which is self similar under magnification. The Cantor middle-thirds set can easily be extended to middle-fifths or middle 1/integers or 1/reals sets.

Concept of the Reverse Cantor Set

What if, per chance, one constructs a set in the same way the Cantor set is constructed, but reverses the operations so that one-third of each subsequent line segment is removed from the ends of each line segment rather than the middle? In other words, during each iteration, each line segment is subdivided into three segments, out of which the two end segments are deleted. If this process is continued until the number of iterations approaches infinity, the length of the middle-third segment approaches zero as it does in the normal Cantor set situation. Just like the Cantor set, the reverse Cantor set can be extended to middle-fifths or middle 1/integers or for that matter, 1/reals sets.

The Reverse Cantor Set behaves quite differently from the normal Cantor set. Instead of reducing to a fractal set of points of measure zero of noninteger dimension of ln 2/ln 3 (Cantor set), the line segment reduces to a point of infinite density resulting in a generalized function (e.g., delta function) for the density and thus allowing it to be used in quantum mechanics rather than in fractals.

Construction of a Rational Delta Function Using the Reverse Cantor Set

The Reverse Cantor set density yields a sequence of delta (δ) functions, called δ-sequences, which are defined on a set of rational numbers (e.g., fraction p/q where p and q are integers) and no irrational or imaginary numbers. Thus, the process of starting from a unit interval [-1/2, 1/2], removing

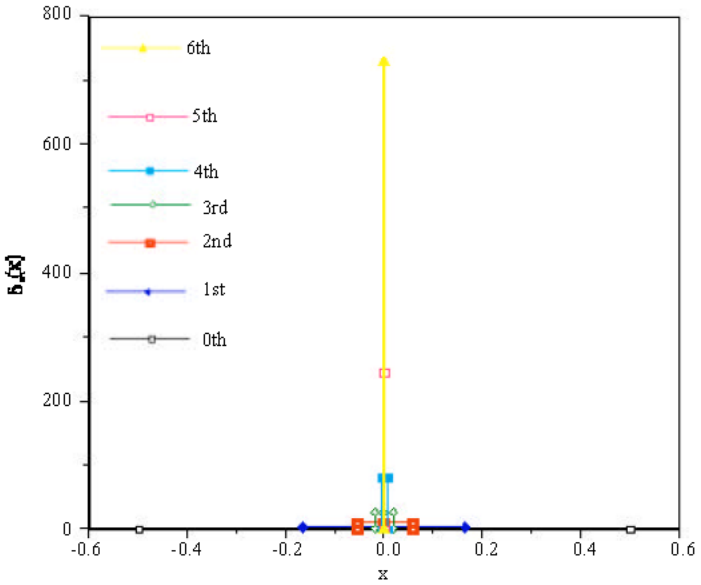

Fig. 1: A graphical representation of the reverse Cantor set based delta function (sequence) $\delta_n(x)$ vs. x

the two end-thirds in subsequent operations or iterations (n) and taking the limit as $n \to \infty$, yields a rational-type δ-function, $\lim_{n\to\infty} \delta_n(x)$. Furthermore, denoting the interval $[-(1/2)3^{-n}, (1/2)3^{-n}]$ to be I_n, $\delta_n(x)$ is defined as follows:

$$\delta_n(x) = 3^n \text{ for } x \in I_n(x), \tag{1a}$$

$$\delta_n(x) = 0 \text{ for } x \notin I_n(x). \tag{1b}$$

The reverse Cantor set density sequence discussed above can be graphed as shown in Fig. 1. The x coordinates represent the length of the subsequent line segments in the set, while the $\delta_n(x)$ coordinate or y coordinate physically represents the density of each line segment. For example, let us assume that the mass of the initial segment of length 1 is 1 g. If we assume a specific unit for the mass of the segment, we might as well assume that the length is also measured in the same unit, such as centimeters. Thus, the density of the initial line segment is 1 g cm^{-1}. Now, let us perform the reverse Cantor operations, removing one-third of this line segment from each end. We will, however, keep the mass constant at 1 g.

This results in the density of the line fragment (3 g cm^{-1}) to be higher than that of the previous segment by a factor of 3. If we keep the mass of each subsequent line section constant at 1 g while decreasing its length, we obtain a graph as shown in Fig. 1, with the length of the line segment becoming very small as the density becomes very high. Graphically, this is represented by the spike protruding upwards from the middle of the x axis (x = 0).

This graph, although it presently models a simple length-density system, looks very similar to the graph of a standard rational delta function (Fig. 5.7.3 of Stenger, 1993). Although the method used by Stenger (1993) involves relatively complicated sinc-like generalized functions, his end result is very similar to the reverse Cantor set density, as is apparent from the similarities of the two graphs. It is interesting to compare the reverse Cantor set density with its Cantor set counterpart. The Cantor set density function is called the devil's staircase (Moon, 1989).

Before proceeding any further, a brief discussion of the rational delta function and of delta functions in general is in order. A delta function is a representation of the orthonormality of the eigenfunctions, which comprise the possible solutions to the wave equation in a particular situation. For example, the Dirac delta function can be graphically represented by a single line stemming from the origin (x = 0) of the x-axis and approaching infinity. The physical representation of this type of delta function is a solution which is unbounded (hence the height of the graph approaches infinity) and an array of possible wave function eigensolutions which theoretically span the entire real (number) line. This is represented by the width of the graph (which approaches zero), thus showing that the possible eigenvalues in this situation are continuous, with solutions having little spacing between each other. Therefore, the Dirac delta function is a representation of the orthonormality of eigenfunctions in the scattering case, or the case in which the wave function does not decay to zero within a finite region (A.3, Appendix, for a more detailed mathematical explanation).

The Dirac delta function is obviously a limiting case for representing orthonormality of eigenfunctions in quantum mechanics. The other extreme situation occurs in the case of a localized wave function where the corresponding eigenvalues are discrete. This situation can be physically represented, e.g., by a particle confined in an infinite well with reflective walls. The particle has no chance of crossing the barriers that surround it. The orthonormality of eigenfunctions representing the solution of the Schrödinger equation in this case, involves the Kronecker delta function. The graph of this function is a line of unit length (support) that attains a unit height within the domain of definition, $I_0(x)$ and zero outside. The meaning for the graph is that possible eigensolutions in this case must have integers as indices and the particle wave does not extend beyond a finite region (A.3, Appendix, for a more detailed explanation of the Kronecker delta function).

Mathematically speaking, the Dirac δ function is a distribution. The corresponding δ sequence is defined on a set of real numbers. The orthonormality condition is, therefore, a Fourier transform — an integral representation. In contrast, the Kronecker δ is a binary, 0 or 1 and is defined on set of integers. The orthonormality condition is, therefore, a Fourier series — a summation representation. The rational δ sequence is defined on a set of rational numbers, which are in between the above two. The orthonormality condition will be shown to be in the form of discrete Fourier transform — a pseudo-integral representation (on rationals).

While the supports of δ functions in the two extreme cases (i.e., Kronecker and Dirac) are either the unit interval or zero, their reverse Cantor set counterparts are all fractions and thus bridge the gap between these two extremes. This phenomenon leads to the possibility that the reverse Cantor set is a candidate for representing the orthonormality of eigenfunctions for more complicated situations where the wave functions of two or more particles interact. Upon hypothesizing that this is indeed the case, we must find a numerical method that will allow us to use the reverse Cantor set to obtain solutions to quantum mechanical problems, namely those that cannot be solved using exact or closed form techniques.

Comparison of the graph of the reverse Cantor set density (Fig. 1) with the graphs representing the rational delta function, Kronecker delta function and Dirac delta function, gives substantial evidence supporting the proposition that the reverse Cantor set density is indeed some kind of delta function, or more precisely, a delta sequence. In what follows, a formal proof of a theorem to that effect is provided:

Theorem 1

Let p and q be arbitrary nonzero integers and p>q. Define the interval $I_n(x)$ to be $[-(q/p)^n/2, (q/p)^n/2]$, where n is an integer. Then $\delta_n(x)$ defined as

$$\delta_n(x) = (p/q)^n \text{ for } x \in I_n(x), \tag{2a}$$

$$\delta_n(x) = 0 \text{ for } x \notin I_n(x), \tag{2b}$$

is a delta sequence.

Proof

This proof follows the approach given in Keener (1995). Consider a test function, $\phi(x)$, which is continuous near $x = 0$.

$$\lim_{n\to\infty} \int_{-\infty}^{\infty} \delta_n(x)\phi(x)dx = \lim_{n\to\infty} \left(\frac{p}{q}\right)^n \int_{-(q/p)^n/2}^{(q/p)^n/2} \phi(x)dx = \phi(0) \tag{3}$$

by virtue of the mean value theorem. It may also be noted that rational numbers are dense in the real line. Therefore, taking the limit is not a problem.

The stark similarities between the graph of the Reverse Cantor set density and the graph of the rational delta function have already been discussed above. Yet, how is the reverse Cantor set density similar to the seemingly contradictory Kronecker delta function and the Dirac delta function? The answer to this question is relatively simple. When the iteration number, n, approaches infinity, $\delta_n(x)$ (height) also approaches infinity while its support, $I_n(x)$, approaches zero (Fig. 1). Therefore, the height of the line approaches $\delta(x)$, the height of the graph denoting the Dirac δ function (in which case the base is zero while the height is infinity) in the limit $n \to \infty$. Similarly, if $n = 0$, $\delta_n(x) = 1$ with the unit interval as its support, which, when appropriately adjusted with integer subscripts, will yield the Kronecker δ function. In addition to the afore-cited formal proof, the reduction of the reverse Cantor set density based delta function, $\delta_n(x)$, to the two limiting cases of quantum mechanics when limits of the reverse Cantor based delta function are taken, as well as visual similarities between the reverse Cantor function and the rational delta function, give convincing evidence that the reverse Cantor set density is indeed a rational delta function.

The reverse Cantor set δ sequence is shown in this study to be a representation of the orthonormality of eigenfunctions of the Schrödinger wave equation for the wave functions of particles which have a probability of appearing far outside the barriers of a well, but not all the way to infinity. When the particle is mostly confined within the well and seldom appears outside, n is small and the reverse Cantor based δ function closely resembles the Kronecker δ function. On the other hand, since a particle invariably appears outside a barrier and its wave function decays to zero very slowly in the scattering case, the reverse Cantor set density with a large n-value can be used as a representation of the orthonormality of the corresponding eigenfunctions. Now let us consider a situation where a well and a barrier are placed close to each other. The particle appears inside and outside the well with relatively same order of frequency and the corresponding wave function decays moderately fast upon transcending the barrier because of the presence of the well. In this case, the orthonormality of eigenfunctions comprising the wave function can best be represented using the reverse Cantor set density, $\delta_n(x)$, with an intermediate value of n. It is interesting to mention here that this concept of a well placed next to a barrier was used by George Gamow in 1928 to explain the enormous variation in the mean life for α decay of radioactive nuclei (Tipler, 1998). Gamow represented the radioactive nucleus by a potential well containing an α particle. Outside the nucleus, the nuclear or strong force is negligible and the potential is described by Coulomb's law.

A New Method for Normalization of the Energy and Momentum Eigenfunctions Based on Reverse Cantor Set Delta Function

Let the wave function, $\psi(\vec{r})$, which is solution to the Schrödinger equation, be expanded in the reverse Cantor set based rational delta function, δ_n as follows:

$$\psi(\vec{r}) = \int_{Rat,n} \psi(\vec{r}')\ \delta_n^3(\vec{r}-\vec{r}')\ d^3\vec{r}', \tag{4}$$

where $\int_{Rat,n}$ denotes a pseudo-integral on rationals and $\delta_n^3(\vec{r})$ is the three-dimensional analog of $\delta_n(x)$ defined in Eq. (1).

Let the momentum eigenfunction whose continuous analog given in the form

$$u_p(\vec{r}) = u_k(\vec{r}) = C\ \exp(i\vec{k}.\vec{r}), \tag{5}$$

satisfy the orthonormality relations both in the position as well as momentum (propagator) space with respect to the reverse Cantor set-based rational delta function, δ_n,

$$\int_{Rat,n} u_k^*(\vec{r}')\ u_k(\vec{r})\ d^3k = \delta_n^3(\vec{r}-\vec{r}'); \tag{6}$$

$$\int_{Rat,n} u_{k'}^*(\vec{r})\ u_k(\vec{r})\ d^3r = \delta_n^3(\vec{k}-\vec{k}'). \tag{7}$$

Substitution of Eq. (6) into Eq. (4) yields

$$\psi(\vec{r}) = \int_{Rat,n} \psi(\vec{r}') \int_{Rat,n} u_k^*(\vec{r}')\ u_k(\vec{r})\ d^3\vec{k}\ d^3\vec{r}' = \int_{Rat,n} A_k\ u_k(\vec{r})\ d^3\vec{k}, \tag{8}$$

where the Fourier transform, A_k, because of Eq. (7) is given by

$$A_k = \int_{Rat,n} u_k^*(\vec{r}')\ \psi(\vec{r}')\ d^3\vec{r}'. \tag{9}$$

As is discussed in the Appendix, Eq. (7) and (6) would, if the Dirac δ function is used in the normalization, give rise to orthonormality conditions, given by Eq. (A.16) and (A.18). However, since the orthonormality relations, given by Eq. (6) and (7) employ the reverse Cantor set based rational delta function, δ_n, Eq. (8) and (9) must be modified as follows. Identifying $I_n(x) = \Delta_n$, n = 0, 1, 2, ... the sampling interval on the x-axis (one-dimensional case), we can express the wave function ψ, given by Eq. (9) in the form of discrete Fourier transform as given below:

$$A_k = \int_{Rat,n} u_k^*(\vec{r}')\ \psi(\vec{r}')\ d^3\vec{r}' = \int_{Rat,n} \psi(\vec{r})\ e^{2\pi i\vec{v}.\vec{r}/(n\Delta_n)}\ d^3\vec{r}, \tag{10}$$

where

$$\vec{k} = 2\pi\vec{v}/(n\Delta_n), \tag{11}$$

with n being the total number of sampling points and $\vec{v} \in Z^3$, the set of integers in three dimensions. It then immediately follows (Press *et al*., 1992) that the Fourier transform, A_k, of the wave function, $\psi(\vec{r})$, can be approximated to its discrete form as follows:

$$A_k = \int_{Rat,n} \psi(\vec{r})\ e^{2\pi i\vec{v}.\vec{r}/(n\Delta_n)}\ d^3\vec{r} \approx (\Delta_n)^3 \sum_{j=0}^{n-1} \psi_j\ e^{2\pi i\vec{v}.\vec{r}_j/(n\Delta_n)} = (\Delta_n)^3 A_k^d \tag{12}$$

In one-dimensional case, this reduces to

$$A_k \approx \Delta_n \sum_{j=0}^{n-1} \psi_j\ e^{2\pi ivj/n} = \Delta_n A_k^d \tag{13}$$

A_k^d in Eq. (12) or (13) represents discrete Fourier transform, while A_k is the continuous Fourier transform when viewed as samples of a continuous function sampled at an interval of A_k^d.

The inverse discrete Fourier transform, which recovers the sampled, $\psi_i = \psi(\vec{r}_j)$ from discrete Fourier transform, A_k^d, is, in the one-dimensional case, given by

$$\psi_j = \frac{1}{n} \sum_{j=0}^{n-1} A_k^d \, e^{-2\pi i vj/n} \tag{14}$$

The Fast Fourier Transform (FFT) is an algorithm that computes in $O(N \log_2 N)$ operations as compared to the DFT's $O(N^2)$. The Discrete Wavelet Transform (DWT) is a more recently developed fast computational tool that linearly operates on a data vector, the length of which is an integral power of 2 and transforms it into a numerically different vector without altering the length. Like the FFT, the DWT is invertible and orthogonal, its inverse transform, when viewed as a large matrix, being the transpose of the transform. Both the FFT and DWT can, therefore, be viewed as rotations in function space, from the input space to a new domain. In the case of FFT, the rotated domain has basis functions in the form of standard sines and cosines, while in the wavelet domain the basis functions are somewhat novel, with names like mother functions and wavelets. The details of the FFT and DWT algorithms are available in Press *et al*. (1992) and will not be repeated here.

An Example Problem from Solid State Physics

In order to test the applicability of the present novel technique, the following problem from solid state physics/materials science is considered. Let us consider some real situation; e.g., conduction of electricity through a commercial quality copper wire of finite length, which is nothing but motion of free (outer) electrons inside the metal wire. The metal wire of finite length is idealized as an infinite (one-dimensional) square well, partly because this is one of the easiest problems to solve using the time-independent Schrödinger equation (also known as problem of a particle in the box) and in part, because this potential is a relatively good approximation of the motion of a free electron inside a metal. For this problem the potential energy is of the form (Tipler, 1998):

$$V(x) = 0, \qquad -L < x < L \tag{15a}$$

$$V(x) = \infty, \qquad x < -L \text{ or } x > L \tag{15b}$$

It may, however, be noted that the commercial quality copper wire usually contains a variety of impurities or contaminants, most notably oxides of the metal, which are insulators and serve as barriers. This is modeled here as one-dimensional square potential barrier of thickness a. For the barrier, the potential energy, V_b, is of the form (Schiff, 1968):

$$V_b(x) = 0, \qquad x < 0 \text{ and } x > a \tag{16a}$$

$$V_b(x) = V_0, \qquad 0 < x < a \tag{16b}$$

where V_0 is positive and $a << L$. The barrier inside the infinite square well model is shown in Fig. 2.

Although the infinite square potential well and square potential barrier problems have simple closed-form solutions available in text-books, the combined barrier inside the well problem will not admit such simple text-book solutions because of the interaction of the two potentials. It may be noted that the stand-alone square well problem has discrete eigenvalues and the corresponding eigenfunctions are orthonormalized with respect to the Kronecker δ function, while the free-standing square potential

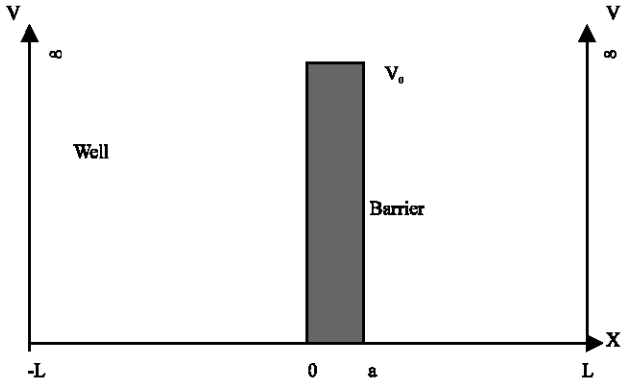

Fig. 2: A schematic representation of a barrier located inside a potential well

barrier problem admits a continuous spectrum of eigenvalues with the corresponding eigenfunctions being orthonormalized with respect to the Dirac δ function. In the former case, the computed wave functions are localized within the box (well), while the latter (scattering) wave function is extended all the way to infinity. However, since in the present barrier inside the box (well) problem, the wave function is permitted neither to extend all the way to infinity, nor to be localized in length scale of the order of barrier thickness, a (<< L), the computed eigenfunctions cannot be orthonormalized with respect to either the Dirac or Kronecker δ functions. Consequently, these eigenfunctions need to be orthonormalized with respect to the present reverse Cantor set based rational δ function. Therefore, the energy eigenvalues for the particle inside the well cannot, in general, be expressed in the form

$$E_n = \frac{\pi^2 \hbar^2 \nu^2}{8\, mL^2}, \nu = 1, 2, 3, \ldots \tag{17}$$

and the correct solution must be of the form of discrete Fourier transform, as given by Eq. (13) and (14).

$$u_j = \frac{1}{n} \sum_{j=0}^{n-1} A_k^d \, e^{-2\pi i \nu j/n}, \tag{18a}$$

$$A_k \approx \Delta_n \sum_{j=0}^{n-1} u_j \, e^{2\pi i \nu j/n} = \Delta_n \, A_k^d, \tag{18b}$$

where u_j is the time independent wave function. A_k with k being the momentum eigenvalue need to be numerically evaluated by using the DFT (or FFT, DWT, etc.) technique and must satisfy the various boundary conditions of the problem. This scheme is currently being implemented and numerical results will be reported in future.

It may be noted, however, for a << |x| < L, Eq. (17) is a reasonable approximation. The corresponding momentum eigenvalue is given by $K = \pi\nu/2L$, $\nu = 1, 2, 3, \ldots$, which can be correlated to the incident particle wave function solution for the barrier problem. The next step involves solving the barrier boundary value problem in the usual manner (Schiff, 1968), which will, of course, be in significant error. However, the fact that the present method reduces to the standard text-book solutions, when the well and the barrier are uncoupled, testifies to the validity and effectiveness of the present method.

CONCLUSIONS

A simple yet novel method for construction of rational delta function using the reverse Cantor set and its application to quantum mechanics is presented. This study is primarily concerned with

formulation of new rational delta function based representation theory for orthonormalization of the computed eigenfunctions — both in the physical space as well as in the Fourier space — which will serve as the basis functions for the wave function, ψ, the solution to the Schrödinger wave equation subjected to prescribed boundary conditions. The fundamental set theoretic basis for formulation of a rational delta function, yielding a Reverse Cantor set density sequence, $\delta_n(x)$, is hitherto unavailable in the literature. This reduces to the Dirac δ-function and Kronecker δ-function in the limiting cases of $n \to \infty$ and $n \to 0$, respectively and thus bridges the gap between the two situations that arise in quantum mechanics, namely bound states with discrete eigenvalues and scattering case with continuous spectrum of eigenvalues.

Most important, this novel rational delta function, $\delta_n(x)$, permits the resulting computed wave function to be expressed in the form of Discrete Fourier Transform (DFT) in the Fourier domain and recover the sampled wave function in the physical domain by employing the Inverse Discrete Fourier Transform (IDFT). The example problem of a barrier inside a well studied here sheds new light on the nature of interaction of two or more potentials and will serve as a prelude to more complex many body interaction problems. The relatively straightforward transition to faster techniques, such as the Fast Fourier Transform (FFT) and Discrete Wavelet Transform (DWT), is currently being implemented and will be reported in the near future.

APPENDIX: RELEVANT BACKGROUND INFORMATION ON QUANTUM MECHANICS

A.1. Basic Interpretive Postulates for Wave Functions

The Schrödinger equation which describes the motion of a particle is written as follows (Schiff, 1968):

$$\frac{\partial}{\partial t}\psi(\vec{r},t) = \left[-\frac{\hbar^2}{2m}\nabla^2 + V(\vec{r},t)\right]\psi(\vec{r},t), \tag{A.1}$$

where $\psi(\vec{r},t)$ represents the wave function, which describes the motion of a particle; m and $\vec{r}$ represent the mass and position vector of a particle, respectively; t denotes the time; $V(\vec{r},t)$ is the time dependent potential energy; $i=\sqrt{-1}$, while ∇^2 is the Laplacian operator and $\hbar = h/(2\pi)$, where h is the Planck constant.

There are three fundamental physical postulates from which a complete interpretation of the wave function, $\psi(\vec{r},t)$, can be derived. The first postulate states that each dynamic variable (observable), such as energy or momentum, that relates to the motion of a particle can be represented by a linear operator. Some important differential operators of interest are energy and momentum operators given by

$$E \to i\hbar\frac{\partial}{\partial t}, \quad \vec{p} \to -i\hbar\vec{\nabla}. \tag{A.2}$$

The second postulate states that one or another of the eigenvalues of the operator is the only possible result of a precise measurement of the dynamic variable represented by the operator. The third postulate is that the number of measurements that result in the eigenvalue is proportional to the square of the magnitude of the coefficient of the eigenfunction expansion of the wave function, ψ.

It may be noted that if the potential energy does not depend on time, the wave function can be separated into a time part and space part as follows:

$$\psi(\vec{r},t) = f(t)u(\vec{r}) \tag{A.3}$$

The above postulates are useful for description of the total energy and momentum of a particle.

EIGENSOLUTION TO TIME INDEPENDENT SCHRÖDINGER EQUATION — ENERGY AND MOMENTUM EIGENFUNCTIONS

Energy Eigenfunction

The energy eigenvalue equation is written as (Schiff, 1968)

$$\left[-\frac{\hbar^2}{2m}\nabla^2 + V(\vec{r})\right] u_E(\vec{r}) = E\ u_E(\vec{r}), \tag{A.4}$$

where E denotes the total energy eigenvalue; $u_E(\vec{r})$ is the corresponding eigenfunction; $V(\vec{r}, t)$ is the time independent potential energy. As is discussed in standard text-books, the energy eigenfunctions, $u_E(\vec{r})$, can be divided into two classes — (i) the localized eigenfunctions that are associated with discrete eigenvalues and (ii) eigenfunctions that are extended to infinity, the corresponding eigenvalues being continuous.

The set of eigenfunctions, $u_E(\vec{r})$, each of which is normalized and orthogonal to one another is called an orthonormal set of functions or basis functions in the sense that an arbitrary wave function can be expanded in terms of them:

$$\psi(\vec{r}) = \sum_E A_E\ u_E(\vec{r}). \tag{A.5}$$

The closure property of the orthonormal set of functions, $u_E(\vec{r})$, is given as follows:

$$\sum_E u_E^*(\vec{r}')\ u_E(\vec{r}) = 0, \quad \vec{r}' \neq \vec{r}, \tag{A.6a}$$

$$\int \sum_E u_E^*(\vec{r}')\ u_E(\vec{r})\ d^3r' = 1, \tag{A.6b}$$

if the volume of integration includes the point $\vec{r}' = \vec{r}$. The superscript * denotes the complex conjugate.

Momentum Eigenfunction

The eigenfunctions of the linear momentum operator -ih∇ provide a very useful example of the conceptual framework of this study. The momentum eigenfunctions are solutions of three eigenvalue equations

$$-i\hbar\ \nabla u_p(\vec{r}) = \vec{p}\ u_p(\vec{r}), \tag{A.7}$$

which are of the form

$$u_p(\vec{r}) = u_k(\vec{r}) = C\ \exp(i\vec{k}.\vec{r}), \tag{A.8}$$

where $\vec{k} = \vec{p}/\hbar$ is called the propagation vector. The corresponding eigenvalues are $\vec{p} = \hbar\vec{k}$. In Eq. (A.8), C is a normalization constant. The momentum eigenvalue is related to the energy eigenvalue discussed above through the relationship,

$$E = \frac{\hbar^2\vec{k}^2}{2m}.$$

Standard Methods for Normalization of the Energy and Momentum Eigenfunctions

The two standard methods for normalization of momentum eigenfunctions are (i) box normalization and (ii) Dirac Delta normalization.

Box Normalization

Both the energy and momentum eigenfunctions can be normalized by restricting their domain to an arbitrarily large but finite box of volume L^3 centered at the origin. The eigenfunctions are subjected to periodic boundary conditions at the walls of the box. It is obvious that $u_k(\vec{r})$, as defined by Eq. (A.8), is normalized if $C = L^{3/2}$. The spacing of the propagating vectors and the corresponding energy eigenvalues can be made as small as desired by making the box dimension arbitrarily large. The limit $L \rightarrow \infty$ can be taken at the end, which corresponds to the case of continuous spectrum of eigenvalues. It can be easily shown that the box normalized momentum eigenfunction given by the relation

$$u_k(\vec{r}) = L^{-3/2} \exp(i\vec{k}.\vec{r}), \tag{A.9}$$

satisfy the orthonormality condition

$$\int u^*_{k'}(\vec{r})\ u_k(\vec{r})\ d^3r = \delta_{kk'}, \tag{A.10}$$

where is $\delta_{kk'}$ the Kronecker delta.

Dirac Delta Normalization

Both the energy and momentum eigenfunctions can easily be normalized using the Dirac delta function, when they are continuous without having to resort to the introduction of a box with periodic boundary conditions. Dirac δ function is defined as follows:

$$\delta(x) = 0 \text{ if } x \neq 0\ ; \qquad \int \delta(x)\ dx = 1. \tag{A.11}$$

An equivalent definition is given as follows (Keener, 1995):

$$\int f(x)\ \delta(x)\ dx = f(0) \tag{A.12}$$

where the integration includes the point x = 0. It then follows that the closure property of the energy eigenfunctions, given by Eq. (A.6) above, reduces to the following orthonormality relation:

$$\sum_E u^*_E(\vec{r}')\ u_E(\vec{r}) = \delta^3(\vec{r} - \vec{r}') \tag{A.13}$$

Another representation of the Dirac δ function is given as follows:

$$\delta(x) = \lim_{g\rightarrow\infty} \frac{\sin(gx)}{\pi x} \tag{A.14}$$

This representation of the Dirac δ function is used to derive orthonormality integral for momentum eigenfunctions without having to impose box normalization. This results in a momentum eigenfunction of the form of Eq. (A.8) over the entire (infinite) space with all real vectors $\vec{k} = \vec{p}/\hbar$ (Schiff, 1968):

$$u_k(\vec{r}) = (8\pi^3)^{-1/2} \exp(i\vec{k}.\vec{r}) \tag{A.15}$$

Orthonormality relation can now be easily obtained as follows:

$$\int u_{k'}^{*}(\vec{r})u_{k}(\vec{r})d^{3}r = \delta^{3}(\vec{k}-\vec{k}') \tag{A.16}$$

It is a well-known fact that the box normalization when taken to the limit $L \to \infty$ reduces to its Dirac δ function based counterpart in a typical problem. $\vec{r}$

$$\sum_{k} u_{k}^{*}(\vec{r}')u_{k}(\vec{r}) \xrightarrow[L\to\infty]{} \delta^{3}(\vec{r}-\vec{r}') \tag{A.17}$$

Furthermore, the closure relation shows that the momentum eigenfunctions are orthonormal with respect to integration over the position vector (Eq. A.16, A.17) as well as with respect to summation or integration over the eigenvalue $\vec{k} = \vec{p}/\hbar$ (as shown below):

$$\int u_{k}^{*}(\vec{r}')u_{k}(\vec{r})d^{3}k = \delta^{3}(\vec{r}-\vec{r}'). \tag{A.18}$$

An arbitrary continuous function $\psi(\vec{r})$ can be expressed in terms of the Dirac δ function as follows:

$$\psi(\vec{r}) = \int \psi(r')\delta^{3}(\vec{r}-\vec{r}')d^{3}r' \tag{A.19}$$

It then follows that in the periodic case (box with periodic boundary conditions giving discrete eigenvalues), can be expanded in Fourier series with either the momentum or energy eigenfunctions as basis functions. Although the mathematical expressions given below pertain to momentum eigenfunctions, similar results follow for the case of energy eigenfunctions.

$$\psi(r) = \int \psi(r')\sum_{k} u_{k}^{*}(\vec{r}')u_{k}(\vec{r})d^{3}r' = \sum_{k} A_{k}u_{k}(\vec{r}), \tag{A.20}$$

where the Fourier coefficients, A_k, are given by

$$A_{k} = \int u_{k}^{*}(\vec{r}')\psi(r')d^{3}r'. \tag{A.21}$$

Similarly, for the aperiodic case (continuous spectrum of eigenvalues), the wave function $\psi(r)$ can be expanded in Fourier integral (transform) as follows:

$$\psi(r) = \int \psi(r')\int u_{k}^{*}(\vec{r}')u_{k}(\vec{r})d^{3}kd^{3}r' = \int A_{k}u_{k}(\vec{r})d^{3}k, \tag{A.22}$$

where A_k is given by Eq. (A.21).

ACKNOWLEDGEMENT

The author gratefully acknowledges the receipt of the following monetary awards — Intel Science Talent Search (STS) semi-finalist award, American Mathematical Society Karl Manger Award and United Technologies Corporation Scholarship — for an earlier version of this work.

REFERENCES

Asker, A., 1981. A finite element method with local trigonometric basis for close coupling equations. J. Chem. Phys., 74: 6133-6143.

Daubechies, I., 1992. Wavelets, S.I.A.M. Soc. Ind. Appl. Math., Philadelphia.

Devaney, R.L., 1989. Chaotic Dynamical Systems, 2nd Edn., Addison-Wesley, Reading, MA.

Feit, M.D. and J.A. Fleck, Jr., 1983. Solution of Schrödinger equation by a spectral method II: Vibrational energy levels of triatomic molecules. J. Chem. Phys., 78: 301-308.

Hoffman, D.K., G.W. Wei, D.S. Zhang and D.J. Khouri, 1998. Interpolating distributed approximating functionals. Phys. Rev. E, 57: 6152-6157.

Keener, J.P., 1995. Principles of Applied Mathematics, Addison-Wesley, Reading, MA.

Kosloff, D. and R. Kosloff, 1983. A Fourier method solution for the time dependent Schrödinger equation as a tool in moleculer dynamics. J. Comp. Phys., 52: 35-53.

Leasure, S.C., K.F. Milfeld and R. Wyatt, 1981. Quantum molecular dynamics in intense laser fields: Theory and applications to diatomic molecules. J. Chem. Phys., 74: 6197-6211.

Lee, S.Y. and E.J. Heller, 1982. Exact time-dependent wave packet propagation: Application to the photodissociation of methyl iodide. J. Chem. Phys., 76: 3035-3044.

Lill, J.V. and D.J., Khouri., 1984. Comparisons of approximate and exact quantal molecule—surface scattering calculations. Chem. Phys. Lett., 112: 249-257.

Mattuck, R.P., 1992. A Guide to Feynman Diagrams in the Many-Body Problem. 2nd Edn., Dover, New York.

Moon, F.C., 1992. Chaotic and Fractal Dynamics, John Wiley and Sons, New York.

Press, W.H., S.A. Teukolsky, W.T. Vettering and B.P. Flannery, 1992. Numerical Recipes in C. 2nd Edn., Cambridge University Press.

Schiff, L.I., 1968. Quantum Mechanics, 3rd Edn., McGraw-Hill, New York.

Sharafeddin, O. and J.Z.H. Zhang, 1993. A DVR based time-dependent wave packet treatment for reactive scattering. Chem. Phys. Lett., 204: 190-196.

Stenger, F., 1993. Numerical Methods Based on Sinc and Analytic Functions. Springer Verlag, New York.

Szabo, A. and N. S. Ostlund, 1996. Modern Quantum Chemistry. Dover, New York.

Tipler, P.A., 1998. Modern Physics. Worth Publishers. New York.

Wolken, Jr., G., 1973. Theoretical studies of atom-solid elastic scattering: He+LiF. J. Chem. Phys., 58: 3047-3064.

Wyatt, R.E., 1995. Matrix spectroscopy: Computation of interior eigenstates of large matrices using layered iteration. Phys. Rev. E, 51: 3643-3658.